

EUROPEAN  
HEMATOLOGY  
ASSOCIATIONFerrata Storti  
Foundation

## Macrophage scavenger receptor SR-AI contributes to the clearance of von Willebrand factor

Nikolett Wohner,<sup>1\*</sup> Vincent Muczynski,<sup>1\*</sup> Amel Mohamadi,<sup>1</sup> Paulette Legendre,<sup>1</sup> Valérie Proulle,<sup>1,2</sup> Gabriel Aymé,<sup>1</sup> Olivier D. Christophe,<sup>1</sup> Peter J. Lenting,<sup>1</sup> Cécile V. Denis<sup>1</sup> and Caterina Casari<sup>1</sup>

**Haematologica** 2018  
Volume 103(4):728-737

<sup>1</sup>Institut National de la Santé et de la Recherche Médicale, UMR\_S 1176, Univ. Paris-Sud, Université Paris-Saclay, 94276 Le Kremlin-Bicêtre and <sup>2</sup>Service d'Hématologie Biologique, Centre Hospitalier Universitaire Bicêtre, Assistance Publique- Hôpitaux de Paris, 94276 Le Kremlin-Bicêtre, France

NW and VM contributed equally to this work.

### ABSTRACT

Previously, we found that LDL-receptor related protein-1 on macrophages mediated shear stress-dependent clearance of von Willebrand factor. In control experiments, however, we observed that von Willebrand factor also binds to macrophages independently of this receptor under static conditions, suggesting the existence of additional clearance-receptors. In search for such receptors, we focused on the macrophage-specific scavenger-receptor SR-AI. von Willebrand factor displays efficient binding to SR-AI (half-maximum binding  $14 \pm 5$  nM). Binding is calcium-dependent and is inhibited by  $72 \pm 4\%$  in the combined presence of antibodies against the A1- and D4-domains. Association with SR-AI was confirmed in cell-binding experiments. In addition, binding to bone marrow-derived murine SR-AI-deficient macrophages was strongly reduced compared to binding to wild-type murine macrophages. Following expression via hydrodynamic gene transfer, we determined ratios for von Willebrand factor-propeptide over von Willebrand factor-antigen, a marker of von Willebrand factor clearance. Propeptide/antigen ratios were significantly reduced in SR-AI-deficient mice compared to wild-type mice ( $0.6 \pm 0.2$  versus  $1.3 \pm 0.3$ ;  $P < 0.0001$ ), compatible with a slower clearance of von Willebrand factor in SR-AI-deficient mice. Interestingly, mutants associated with increased clearance (von Willebrand factor/p.R1205H and von Willebrand factor/p.S2179F) had significantly increased binding to purified SR-AI and SR-AI expressed on macrophages. Accordingly, propeptide/antigen ratios for these mutants were reduced in SR-AI-deficient mice. In conclusion, we have identified SR-AI as a novel macrophage-specific receptor for von Willebrand factor. Enhanced binding of von Willebrand factor mutants to SR-AI may contribute to the increased clearance of these mutants.

### Correspondence:

peter.lenting@inserm.fr

Received: June 25, 2017.

Accepted: December 27, 2017.

Pre-published: January 11, 2018.

doi:10.3324/haematol.2017.175216

Check the online version for the most updated information on this article, online supplements, and information on authorship & disclosures: [www.haematologica.org/content/103/4/728](http://www.haematologica.org/content/103/4/728)

©2018 Ferrata Storti Foundation

Material published in *Haematologica* is covered by copyright. All rights are reserved to the Ferrata Storti Foundation. Use of published material is allowed under the following terms and conditions:

<https://creativecommons.org/licenses/by-nc/4.0/legalcode>.

Copies of published material are allowed for personal or internal use. Sharing published material for non-commercial purposes is subject to the following conditions:

<https://creativecommons.org/licenses/by-nc/4.0/legalcode>,

sect. 3. Reproducing and sharing published material for commercial purposes is not allowed without permission in writing from the publisher.



### Introduction

Mutations in the gene encoding von Willebrand factor (VWF) may generate proteins displaying defects in biosynthesis, secretion and/or clearance. The quintessential representative of VWF clearance mutants is VWF/p.R1205H, also known as the Vicenza variant.<sup>1</sup> This mutation is associated with VWF antigen (VWF:Ag) levels that are usually below 20%, which are most likely due to a 5- to 10-fold reduced circulatory half-life of the mutant protein.<sup>1,3</sup> Since the description of the Vicenza variant, additional mutations in VWF have been found to provoke a reduced survival. Such mutants have been identified by analyzing VWF survival after desmopressin treatment or by determining ratios between VWF propeptide (VWFpp) and VWF:Ag, with elevated VWFpp/VWF:Ag ratios pointing to increased VWF clearance.<sup>4,8</sup>

The mechanism by which mutations provoke accelerated clearance is poorly understood. Recently, we showed that gain-of-function mutations in the VWF A1 domain induce spontaneous binding to the clearance receptor LDL-receptor related protein-1 (LRP1).<sup>9</sup> In addition, truncation of its N-glycans accelerates LRP1-mediated

ed uptake by macrophages.<sup>10,11</sup> This is in contrast to non-modified VWF, which only binds to macrophage-expressed LRP1 when exposed to increased shear stress.<sup>12</sup> Apart from LRP1, other receptors have also been described to contribute to VWF clearance, including asialoglycoprotein receptor, CLEC4M and Siglec-5.<sup>13-16</sup>

Despite the various receptors having been identified, their functional absence is usually associated with a mild-to-modest effect on VWF clearance. We previously observed that the majority of VWF is targeted to macrophages, and that chemical depletion of macrophages results in a 2- to 3-fold increase in VWF levels.<sup>17,18</sup> We therefore explored the hypothesis that macrophages express one or more additional receptors that contribute to VWF clearance. Here, we present data that are compatible with the macrophage-specific receptor Scavenger receptor class A member I (SR-AI) being a clearance-receptor for VWF. Moreover, we show that two clearance mutants (VWF/p.R1205H and VWF/p.S2179F) display enhanced binding to SR-AI, providing a potential explanation for their reduced half-life in the circulation.

## Methods

### Ethics statement

Animal housing and experiments were done as recommended by French regulations and the experimental guidelines of the European Community. This project was approved by the local ethical committee CEEA 26 (# 2012-036).

### Proteins

A detailed description of the proteins used in this study is provided in the *Online Supplementary Material*. The main proteins included plasma-derived (pd)-VWF purified from VWF concentrates (Wilfactin) and recombinant full-length VWF [wild-type (wt)-VWF, VWF/p.R1205H, VWF/p.V1316M, and VWF/p.S2179F] produced in stably transfected BHK-furin cells using serum-free medium. All variants displayed a similar distribution of multimers (*data not shown*). Non-purified cell culture supernatants were used for protein- and cellular binding experiments. Other proteins are detailed in the *Online Supplementary Material*.

### Cell culture

Detailed information on cell cultures is provided in the *Online Supplementary Material*. Briefly, human macrophages were differentiated from the THP1 acute monocytic leukemia cell line using phorbol 12-myristate 13-acetate, human macrophage colony-stimulating factor and human granulocyte-macrophage colony-stimulating factor as described elsewhere.<sup>18,19</sup> Non-transfected and stable HEK293 cell lines expressing human SR-AI were cultured as described previously.<sup>19</sup> Murine macrophages were obtained from CD115<sup>+</sup> cells as described by Breslin *et al.*<sup>20</sup>

### Cellular binding experiments

A detailed description of cellular binding experiments is provided in the *Online Supplementary Material*. Briefly, cells seeded on glass coverslips were incubated with purified pd-VWF (10 µg/mL) for 1 h at 37°C. Where indicated, culture medium containing recombinant wt-VWF, VWF/p.R1205H, VWF/p.V1316M or VWF/p.S2179F was used. In other experiments, pd-VWF was pre-incubated with monoclonal antibodies to VWF (MAb723 and MAb540, 167 µg/mL) for 30 min at room temperature. Following incubation, cells were gently washed twice and then fixed for 15 min with 4% paraformaldehyde at 37°C.

## Microscopy analyses and immunofluorescence-based quantification

A detailed description of the microscopic analysis is provided in the *Online Supplementary Material*. Briefly, after saturation of non-specific binding sites, cells were exposed to primary antibodies for 2 h at room temperature, followed by incubation for 1 h with secondary antibodies. Nuclei were counterstained with 4',6'-diamidino-2-phenylindole. Alexa-Fluor647 or Alexa-Fluor488-labeled phalloidin was used to determine cell boundaries.

For the Duolink-Proximity Ligation Assay (Duolink-PLA) to detect close proximity between different proteins, double immunostaining was performed as described above with the second antibodies replaced by PLA probes (Sigma-Aldrich). The remainder of the protocol was conducted according to the manufacturer's recommendations and the 550 nm wavelength detection kit was used. Hybridization between the two PLA probes leading to the fluorescent signal only occurs when the distance between the two detected antigens is less than 40 nm.

Images were analyzed using ImageJ software for quantification of fluorescence by measuring the total pixel intensity per cell. Duolink-PLA experiments were analyzed using BlobFinder software (Uppsala University, Sweden) to quantify the number of fluorescent spots per cell. All images were assembled using ImageJ software.

### Immunosorbent binding assay

Binding experiments are described in detail in the *Online Supplementary Material*.

### Mice

Wild-type C57Bl/6 mice were purchased from Janvier Labs (Le Genest-Saint-Isle, France) and SR-AI-deficient C57Bl/6 mice (B6.Cg-*Msrtn1<sup>Csk</sup>/J*) were from The Jackson Laboratory (Bar Harbor, ME, USA). Wild-type mice and SR-AI-deficient mice were not true littermates. MacLRP1-positive and macLRP1-deficient mice were described previously.<sup>12</sup> MacLRP1 mice have a C57Bl/6 background, with >12 backcross steps.

### von Willebrand factor propeptide to antigen ratios

cDNA encoding human wild-type VWF, mutant VWF/p.R1205H or mutant VWF/p.S2179F was cloned into the pLIVE-plasmid (Mirus Bio LLC, Madison, WI, USA) and expressed in wild-type, macLRP1 and/or SR-AI-deficient mice following hydrodynamic gene transfer, essentially as described elsewhere.<sup>9, 21-23</sup> Four days after injection, blood samples were taken via retro-orbital puncture and plasma was prepared for the analysis of VWF propeptide (VWFpp; cat# MW1939; Sanquin Blood Supply, Amsterdam, the Netherlands) and VWF:Ag (in-house enzyme-linked immunosorbent assay using a pool of monoclonal murine anti-VWF antibodies). Both assays are specific for human VWFpp and VWF:Ag, and do not detect murine proteins. VWF:Ag levels varied between 300% and 800% of normal for all constructs. VWF clearance remains unsaturated by VWF levels up to 1500%. The presence of endogenous VWF in the mouse strains used in this study does, therefore, leave clearance of hepatocyte-expressed human VWF unaffected.

## Results

### von Willebrand factor binds to macrophages in an LRP1-independent manner

Previously, we demonstrated that VWF binds to LRP1 in a shear-stress-dependent manner or when it contains type 2B gain-of-function mutations.<sup>9,12</sup> This specific binding was

addressed in Duolink-PLA experiments using THP1-derived macrophages. This assay is positive when a receptor/ligand pair is within a 40-nm radius. As expected, no red spots above background levels could be detected when wt-VWF was analyzed for binding to LRP1, whereas numerous red spots became apparent when THP1-macrophages were incubated with the VWF-type 2B mutant VWF/p.V1316M (Figure 1A-C). This difference was confirmed when quantifying fluorescent signals (Figure 1D; n=5). In control experiments, we also stained THP1-macrophages in a classical manner for the presence of VWF. Interestingly, for those cells incubated with pd-

VWF, the majority of cells proved positive for the presence of VWF (Figure 1E,F). A similar binding of VWF was observed when human macrophages derived from circulating blood precursors were used (*data not shown*). These data indicate that VWF is able to interact with macrophages also in an LRP1-independent manner, even under static conditions. Apparently, receptors other than LRP1 are present on macrophages that mediate binding of VWF.

**Macrophage-specific receptor SR-AI as a potential receptor for von Willebrand factor**

In search for alternative receptors for VWF, we explored

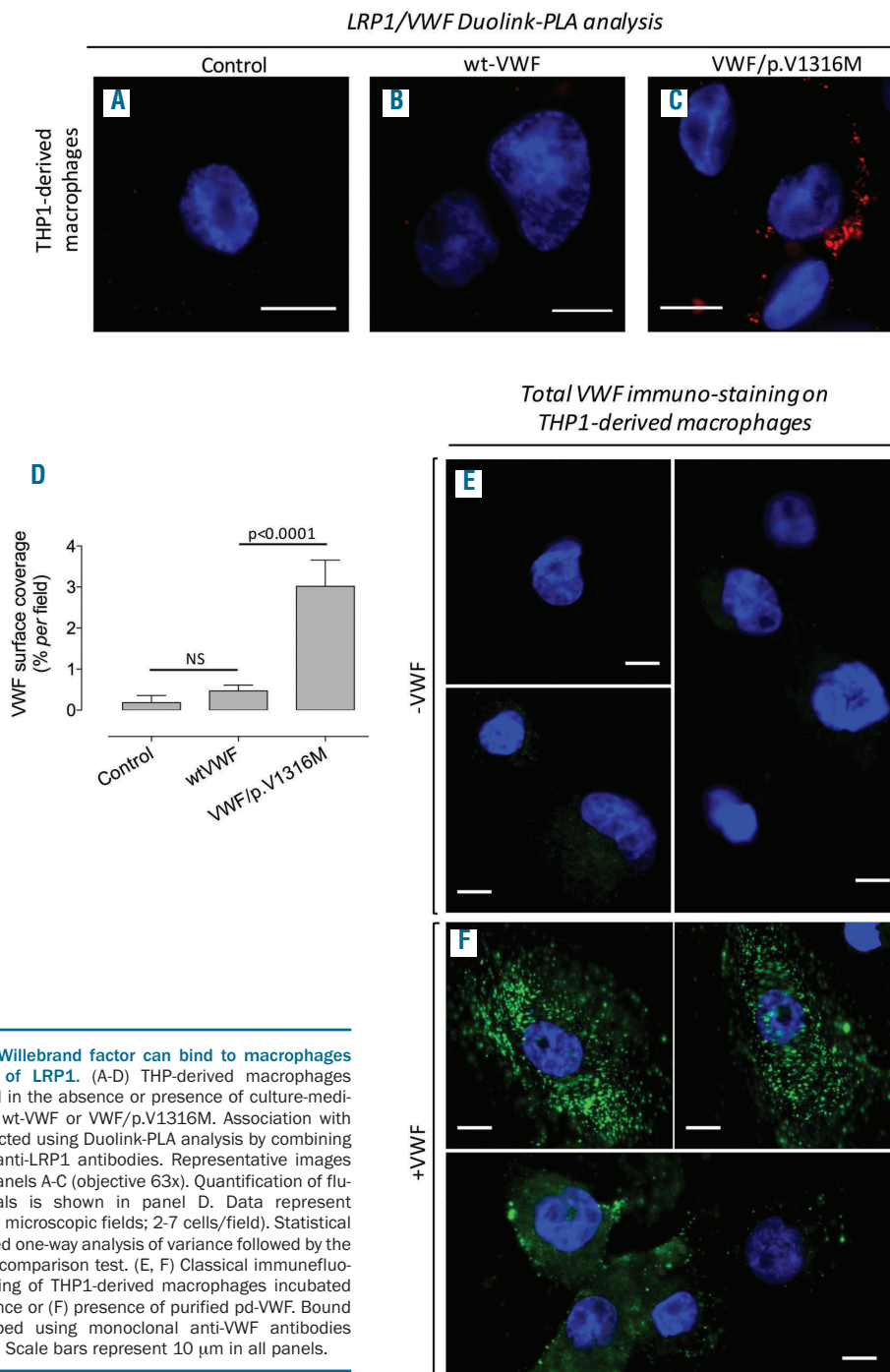


**Figure 1. von Willebrand factor can bind to macrophages independently of LRP1.** (A-D) THP1-derived macrophages were incubated in the absence or presence of culture-medium containing wt-VWF or VWF/p.V1316M. Association with LRP1 was detected using Duolink-PLA analysis by combining anti-VWF and anti-LRP1 antibodies. Representative images are shown in panels A-C (objective 63x). Quantification of fluorescent signals is shown in panel D. Data represent mean±SD (n=5 microscopic fields; 2-7 cells/field). Statistical analysis involved one-way analysis of variance followed by the Tukey multiple comparison test. (E, F) Classical immunofluorescence staining of THP1-derived macrophages incubated in the (E) absence or (F) presence of purified pd-VWF. Bound VWF was probed using monoclonal anti-VWF antibodies (objective 40x). Scale bars represent 10 µm in all panels.

the option that SR-AI could be one of these receptors. SR-AI (also known as SCARA1 or CD204) is specifically expressed on macrophages and is structurally related to SCARA5, an epithelial cell-specific receptor that was identified in genome-wide association studies to be linked to VWF plasma levels.<sup>24</sup> We first analyzed binding of VWF to the soluble extracellular domain of SR-AI (sSR-AI) in an immunosorbent-based assay. Whereas no binding of VWF to albumin-coated control wells was observed, VWF displayed saturable and dose-dependent binding to immobilized sSR-AI (half-maximal binding  $3.5 \pm 1.2 \mu\text{g/mL}$  corresponding to  $14 \pm 5 \text{ nM}$ ;  $n=5$ ) (Figure 2A). We next assessed

the capacity of sSR-AI to interact with various immobilized VWF fragments. sSR-AI bound dose-dependently to each of the three VWF fragments tested (the recombinant D'D3 and A1-A2-A3 regions and the D4/Fc fragment) (Figure 2B), suggesting that the interaction with SR-AI involves different regions of the VWF molecule. Further experiments showed that the A1 domain mediated binding of the A1-A2-A3 fragment to sSR-AI, while both the A2 and A3 domains were incapable of associating with sSR-AI (Figure 2C). In addition, incorporation of the VWD-type 2B mutation VWF/p.V1316M left binding of the A1-domain to sSR-AI unaffected (Figure 2C). Binding

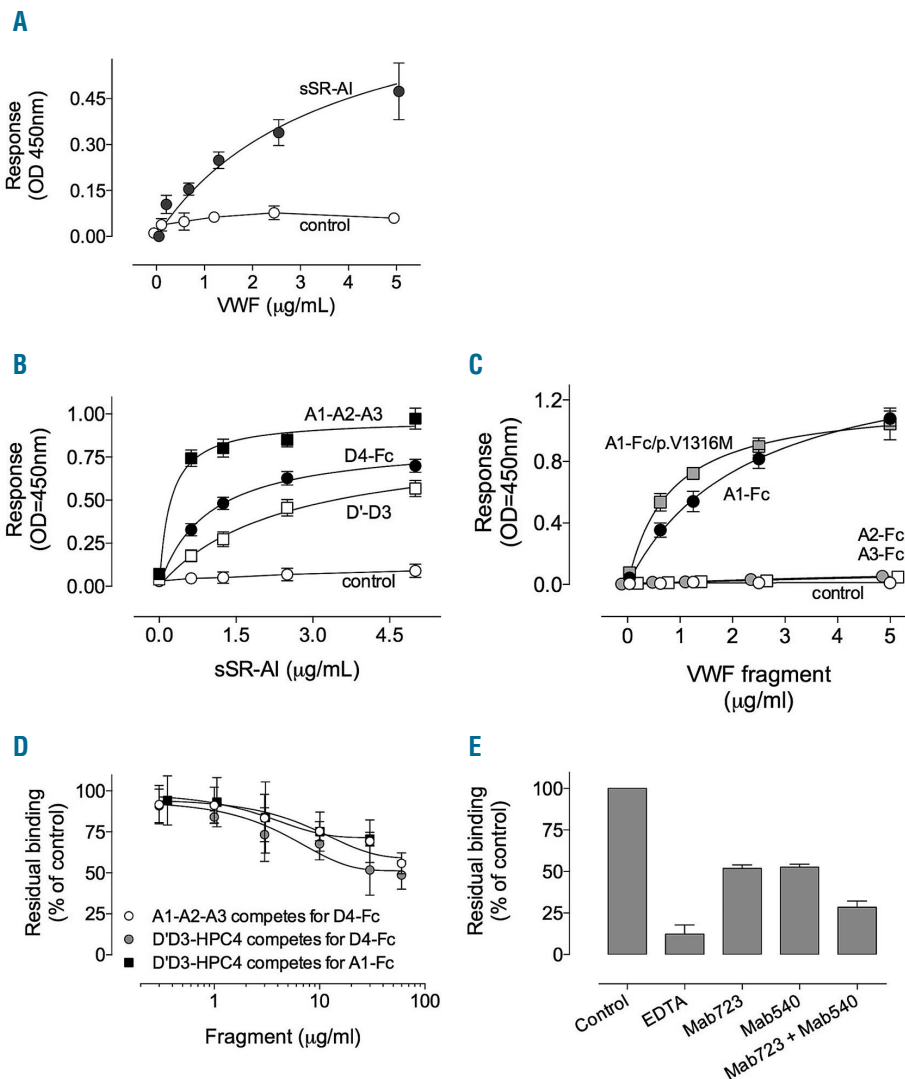


**Figure 2. von Willebrand factor interacts with SR-AI via multiple interactive sites.** (A) Wells coated with recombinant human sSR-AI (closed circles) or bovine serum albumin (BSA) (open circles) were incubated with various concentrations of purified pd-VWF (0–5  $\mu\text{g/mL}$ ). Bound VWF was probed with peroxidase-labeled polyclonal anti-VWF antibodies. (B) Wells coated with recombinant VWF-fragments (closed squares: A1-A2-A3 domain; closed circles: D4-domain fused to Fc fragment; open squares: D'D3 domains) or BSA (control; open circles) were incubated with various concentrations of sSR-AI (0–5  $\mu\text{g/mL}$ ). Bound sSR-AI was probed using biotinylated polyclonal anti-SR-AI antibodies followed by peroxidase-labeled streptavidin. (C) Wells coated with sSR-AI were incubated with various concentrations (0–5  $\mu\text{g/mL}$ ) of recombinant VWF-fragments (closed circles: A1-Fc; gray squares: A1-Fc/p.V1316M; gray circles: A2-Fc; open squares: A3-Fc). Bound fragments were probed using peroxidase-labeled polyclonal anti-human Fc antibodies. Control represents binding of A1-Fc to BSA-coated wells (control; open circles). Other fragments gave similar background signals. (D) sSR-AI-coated wells were incubated with recombinant D4-Fc fragment in the presence of various concentrations of recombinant A1-A2-A3 fragment (open circles) or recombinant D'D3 fragment (gray circles). Alternatively, sSR-AI-coated wells were incubated with recombinant A1-Fc fragment in the presence of various concentrations of recombinant D'D3 fragment (closed squares). Bound fragments were probed using peroxidase-labeled polyclonal anti-human Fc antibodies. (E) sSR-AI-coated wells were incubated with VWF (2.5  $\mu\text{g/mL}$ ) in the absence or presence of EDTA (10 mM), monoclonal anti-VWF antibody Mab723 or Mab540 (25  $\mu\text{g/mL}$ ) or with both antibodies simultaneously (25  $\mu\text{g/mL}$  each). Bound VWF was probed using peroxidase-labeled polyclonal anti-VWF antibodies. For all panels, bound antibodies were detected via TMB-hydrolysis. Data represent mean  $\pm$  SD ( $n=3-5$ ).



of wt-VWF to SR-AI was also not altered upon incubation with ristocetin or botrocetin, indicating that binding does not require VWF to be in its platelet-binding conformation (*data not shown*). Interestingly, we detected little competition between fragments (Figure 2D), suggesting that each domain binds to a distinct site within SR-AI, which at best overlap with each other.

SR-AI function is partially cation-dependent,<sup>25</sup> and we therefore assessed binding of VWF in the presence of EDTA. This revealed that binding of VWF to SR-AI was reduced by 88±6% in the presence of EDTA (Figure 2E). Specificity was further investigated by testing the effect of monoclonal antibodies targeting VWF. We identified two antibodies (*i.e.* Mab723 and Mab540, directed against the A1 and D4 domain, respectively) that each partially inter-

fered with the binding of VWF to sSR-AI (48±2% and 47±2% inhibition by Mab723 and Mab540, respectively; n=3) (Figure 2E). A combination of both antibodies reduced binding by 72±4% (n=4; Figure 2E). Thus, purified VWF interacts in a specific manner with SR-AI and several domains of the VWF molecule contribute to this interaction.

#### von Willebrand factor binds to cellular SR-AI

We next tested whether VWF was able to bind cell-surface exposed SR-AI. First, binding of VWF to non-transfected or SR-AI-transfected HEK293 cells was examined. Whereas no VWF staining could be detected on non-transfected HEK293 cells, clear VWF staining was present on SR-AI-expressing HEK293 cells (Figure 3A-D). High-reso-

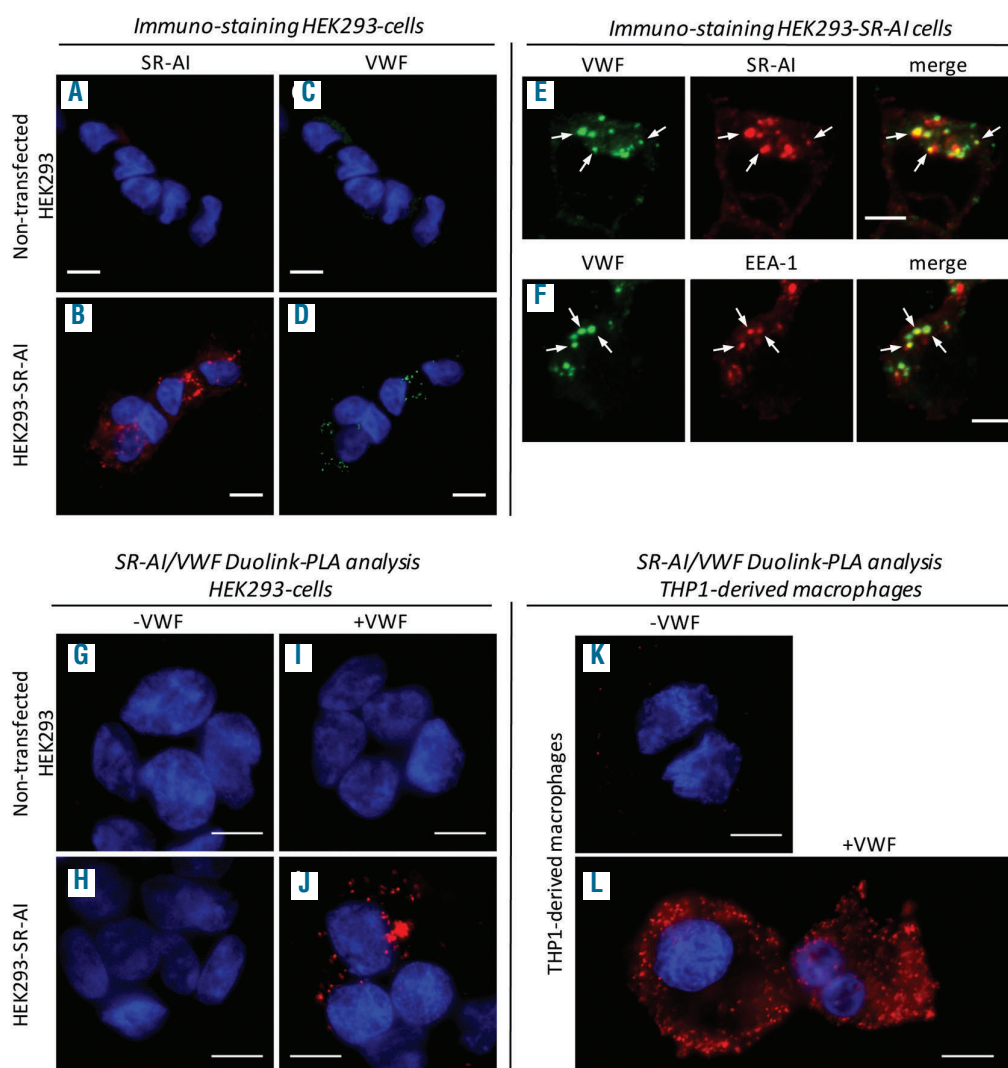


**Figure 3. Binding of von Willebrand factor to SR-AI-expressing cells.** (A-D) Non-transfected (A&C) and hSR-AI-transfected HEK293-cells (B&D) were incubated with purified pd-VWF (10 µg/mL). hSR-AI and bound VWF were probed using polyclonal anti-hSR-AI (red, A&B) and anti-VWF antibodies (green, C&D). Images were obtained via widefield microscopy (objective 40x; scale bars: 10 µm). (E-F) Spinning disk microscopy images (objective 63x; scale bars: 5 µm, z-depth 0.5 µm) of hSR-AI-transfected HEK293-cells incubated with pd-VWF (10 µg/mL). Cells were probed for VWF and hSR-AI (E, green and red, respectively) and for VWF and EEA-1 (F, green and red, respectively). Arrows indicate areas of overlapping signals. (G-J) Non-transfected and SR-AI-transfected HEK293 cells were incubated in the absence or presence of pd-VWF (10 µg/mL). Association with SR-AI was detected using Duolink-PLA analysis by combining anti-VWF and anti-SR-AI antibodies. (K-L) THP1-derived macrophages were incubated in the absence or presence of pd-VWF (10 µg/mL). Association with SR-AI was detected using Duolink-PLA analysis by combining anti-VWF and anti-SR-AI antibodies. Panels G to L: objective 63x; scale bars: 10 µm.

lution analysis revealed that VWF co-localized with SR-AI on these cells (Figure 3E). Moreover, we also observed VWF present in EEA-1-containing endosomes (Figure 3F), indicating that SR-AI binding is followed by uptake and delivery to the lysosomal degradation pathway. Duolink-PLA analysis was performed to further confirm that VWF associates with SR-AI. This analysis revealed numerous red spots when VWF was incubated with SR-AI-expressing HEK293 cells, whereas such spots were absent upon incubation with non-transfected cells or when VWF was omitted from the incubation (Figure 3G-J). A similar colocalization between VWF and SR-AI was observed when testing the binding of VWF to THP1-macrophages (Figure 3K-L). Furthermore, binding to THP1-derived

macrophages was reduced to near background levels when VWF was incubated in the presence of anti-VWF antibodies Mab723 and Mab540 (Figure 4A-C). Finally, we analyzed binding of VWF to primary bone marrow-derived macrophages obtained from wt- and SR-AI-deficient mice. We observed strongly reduced VWF staining to macrophages derived from SR-AI-deficient mice compared to macrophages derived from control mice (Figure 4D-F). Duolink-PLA analysis revealed the formation of red spots, representing complexes between human VWF and murine SR-AI on wild-type macrophages but not on macrophages from SR-AI-deficient mice (Figure 4G,H). From these observations it is conceivable that SR-AI acts as a macrophage-receptor for VWF.

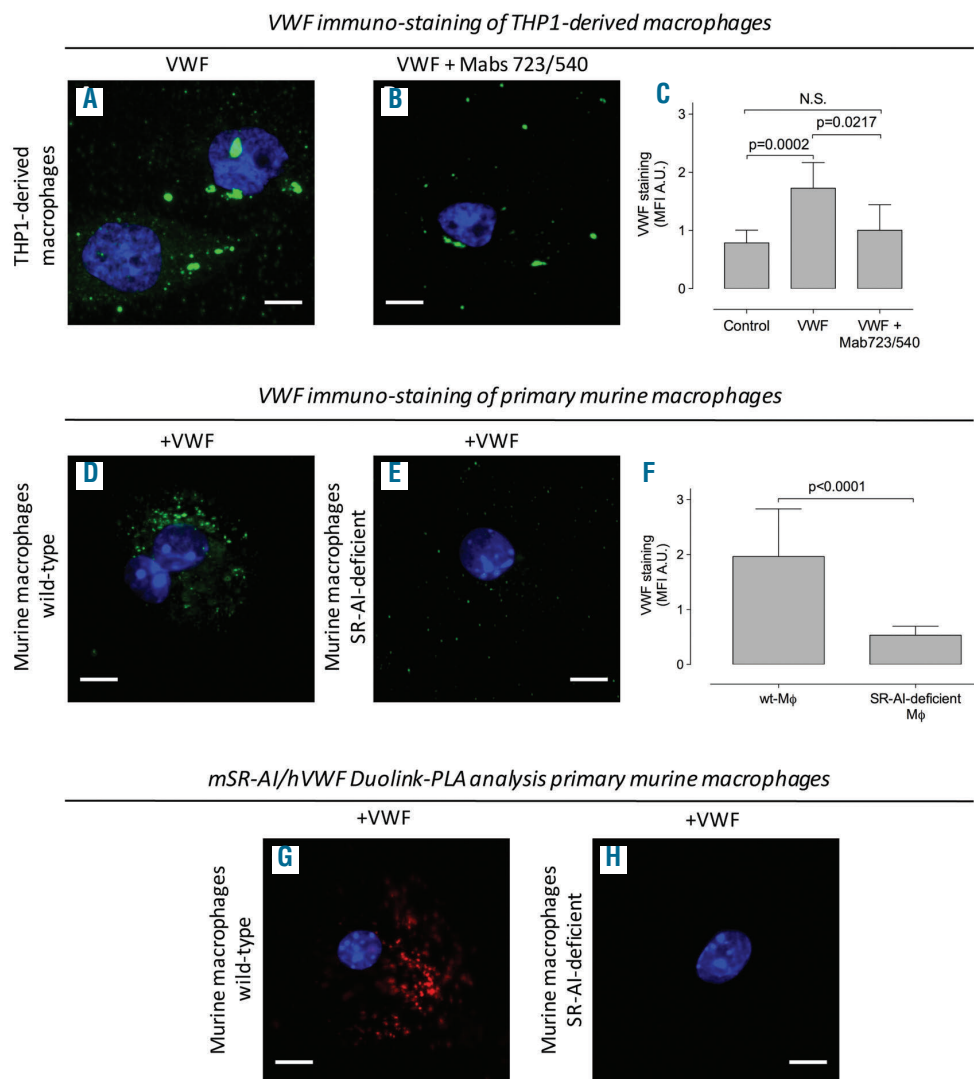


**Figure 4. van Willebrand factor binding to macrophages is reduced by anti-VWF antibodies or SR-AI deficiency.** (A, B) Representative images of THP1-derived macrophages incubated with pd-VWF (10  $\mu\text{g}/\text{mL}$ ) in the absence or presence of monoclonal anti-VWF antibodies Mab723 & Mab540 (167  $\mu\text{g}/\text{mL}$ ). (D, E) Representative images of murine CD115<sup>+</sup> bone marrow-derived macrophages obtained from wt- or SR-AI-deficient mice that were incubated with pd-VWF (10  $\mu\text{g}/\text{mL}$ ). Cell-bound VWF was probed using polyclonal anti-VWF antibodies. (C and F) Quantification of immune fluorescent signals for VWF. Data represent mean  $\pm$  SEM [(n = 64-120 cells (C); n = 62-118 cells (F)]. Statistical analysis involved a one-way analysis of variance with the Tukey multiple comparison test (C) or a two-tailed Mann-Whitney test (F). (G, H) wt and SR-AI-deficient murine-macrophages (CD115<sup>+</sup>) were incubated with human pd-VWF (10  $\mu\text{g}/\text{mL}$ ). Association between murine-SR-AI and human-VWF was detected using Duolink-PLA analysis by combining monoclonal anti-human-VWF and goat anti-murine-SR-AI antibodies. All microscopy figures: objective 40x, scale bars 10  $\mu\text{m}$ .

**von Willebrand factor propeptide to antigen ratio is lower in SR-AI-deficient mice than in wild-type and maLRP1-deficient mice**

To assess the physiological relevance of SR-AI in regulating VWF clearance, we opted to express human VWF in wild-type, maLRP1- and SR-AI-deficient mice via hydrodynamic gene transfer, and to determine the ratio between VWFpp and VWF:Ag, a measure of VWF clearance. As reported previously,<sup>9</sup> VWFpp/VWF:Ag ratios were slightly, but significantly reduced in maLRP1-deficient mice compared to wt-mice ( $1.3 \pm 0.1$  versus  $1.1 \pm 0.1$  for wt- and maLRP1-deficient mice, respectively;  $n=8-9$ ;  $P=0.0114$ ) (Figure 5). This confirms that LRP1 contributes to a modest extent to the clearance of VWF. Interestingly, VWFpp/VWF:Ag levels were even further reduced in SR-AI-deficient mice:  $0.6 \pm 0.2$  versus  $1.3 \pm 0.3$  ( $n=9-14$ ;  $P<0.0001$ ) (Figure 5). VWF is apparently cleared less rapidly in SR-AI-deficient mice than in maLRP1-deficient mice. This suggests that SR-AI plays a more dominant role than that of LRP1 in basal VWF clearance.

**Clearance mutants VWF/p.R1205H and VWF/p.S2179F show enhanced binding to SR-AI**

Given the involvement of the D'D3 and D4 domains in SR-AI binding (Figure 2), it was of interest to investigate whether clearance mutations in these domains affect the interaction with SR-AI. We first analyzed binding of VWF/p.R1205H (the Vicenza variant with a mutation in the D3 domain) and VWF/p.S2179F (with a mutation in the D4 domain) to sSR-AI in an immunosorbent assay. Whereas the interactions of type 2B mutant VWF/p.V1316M and wt-VWF with sSR-AI were similar (half-maximal binding at  $3.1 \pm 0.7$  and  $3.6 \pm 0.9$   $\mu\text{g/mL}$ , respectively), both mutants VWF/p.R1205H and VWF/p.S2179F proved more efficient in interacting with SR-AI ( $1.7 \pm 0.3$  and  $2.3 \pm 0.4$   $\mu\text{g/mL}$ ;  $P=0.0124$ ) (Figure 6A). We then visualized binding of both mutants to SR-AI expressed on THP1-macrophages using Duolink-PLA analysis. Bright red spots were observed for mutants VWF/p.R1205H and VWF/p.S2179F, indicating that both

mutants interact with SR-AI at the macrophage cell surface (Figure 6B-D). Quantitative analysis revealed that fluorescence was significantly increased for both mutants compared to wt-VWF. VWF surface coverage was  $3.2 \pm 0.9\%$  for wt-VWF,  $8.7 \pm 2.4\%$  for VWF/p.R1205H and  $11.6 \pm 2.1\%$  for VWF/p.S2179F (Figure 6E). These data indicate enhanced binding of clearance mutants VWF/p.R1205H and VWF/p.S2179F to SR-AI.

**Increased clearance of mutants VWF/p.R1205H and VWF/p.S2179F is partially corrected in SR-AI-deficient mice**

We next investigated to what extent clearance of the mutants VWF/p.R1205H and VWF/p.S2179F is SR-AI-dependent. Hydrodynamic gene transfer was applied to

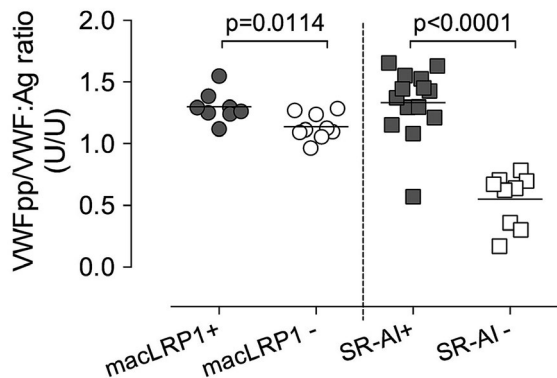
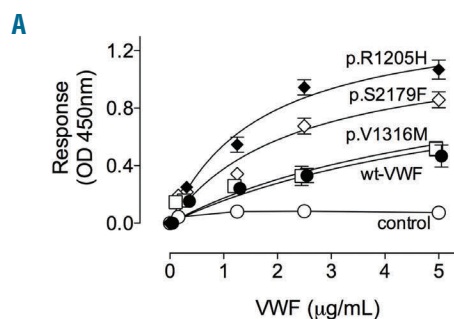


**Figure 5. Deficiency of SR-AI results in decreased VWFpp/VWF:Ag ratios.** Human-wt-VWF was expressed in maLRP1<sup>-</sup> and SR-AI-expressing mice and in maLRP1-deficient and SR-AI-deficient mice following hydrodynamic gene transfer. Four days after injection, plasma samples were prepared for the analysis of VWFpp and VWF:Ag. Assays for VWFpp and VWF:Ag quantify only human VWF expressed via hydrodynamic gene transfer, and do not cross-react with endogenous murine VWF. VWFpp/VWF:Ag ratios for each individual mice included in the study are plotted. Data from maLRP1-mice and SR-AI-mice were compared in a pairwise manner using a two-tailed Student t-test.



SR-AI/VWF Duolink-PLA analysis THP1-derived macrophages

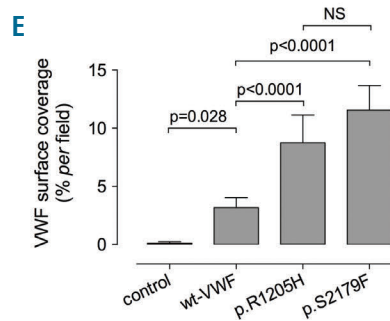
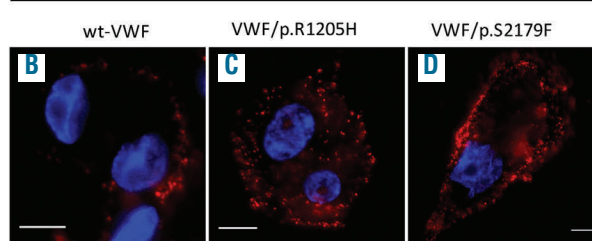


**Figure 6. Enhanced binding of von Willebrand factor mutants p.R1205H and p.S2179F to SR-AI.** (A) Wells coated with sSR-AI were incubated with various concentrations of non-purified recombinant VWF (0-5  $\mu\text{g/mL}$ ). Closed circles: wt-VWF; open squares: p.V1316M; open diamonds: p.S2179F; closed diamonds: p.R1205H. Open circles represent binding of wt-VWF to bovine serum albumin-coated wells. Mutants gave similar background signals. Bound VWF was probed with peroxidase-labeled polyclonal anti-VWF antibodies. All mutants reacted similarly with these polyclonal antibodies. Data represent mean $\pm$ SD ( $n=3$ ). (B-E) THP1-derived macrophages were incubated in the absence or presence of non-purified recombinant wt-VWF (B) or mutants VWF/p.R1205H (C) or VWF/p.S2179F (D). Association with SR-AI was detected using Duolink-PLA analysis by combining anti-VWF and anti-SR-AI antibodies (Objective 63x; scale bars 10  $\mu\text{m}$ ). (E) Quantification of fluorescent signals. Data represent mean $\pm$ SD ( $n=5$  microscopic fields; 2-5 cells/field). Statistical analysis involved one-way analysis of variance followed by the Tukey multiple comparison test.



express human VWF, VWF/p.R1205H and VWF/p.S2179F in control mice and SR-AI-deficient mice, and the VWFpp/VWF:Ag ratio was determined. VWFpp/VWF:Ag ratios were markedly increased for both mutants in control mice [ $2.9 \pm 0.2$  (n=8) and  $4.4 \pm 0.5$  (n=7), for VWF/p.R1205H and VWF/p.S2179F, respectively;  $P < 0.001$  compared to wt-VWF] (Figure 7), confirming that both mutations induce increased clearance of VWF. When expressed in SR-AI-deficient mice, a significant reduction in VWFpp/VWF:Ag ratio was found for both mutants:  $2.0 \pm 0.4$  and  $2.3 \pm 0.5$ , for VWF/p.R1205H and VWF/p.S2179F, respectively ( $P < 0.0001$ ) (Figure 7). These data point to mutants VWF/p.R1205H and VWF/p.S2179F being cleared less rapidly in SR-AI-deficient mice than in wt-mice, suggesting that SR-AI contributes to the clearance of these mutants.

## Discussion

Sinusoidal endothelial cells and macrophages have been proposed to mediate clearance of VWF, with macrophages being particularly dominant.<sup>14,17,26,27</sup> The molecular basis by which macrophages interact with VWF is, however, unclear. Previously, it was reported that VWF is a ligand for the scavenger-receptor LRP1, which is abundantly present on macrophages.<sup>11,12,26</sup> Nonetheless, VWF only interacts with LRP1 when exposed to increased shear stress, or is otherwise in its active conformation, e.g. following incubation with ristocetin or botrocetin, or when harboring a VWD-type 2B mutation. In addition, modulation of the glycan structures in the A2 domain also favors spontaneous binding to LRP1.<sup>10,11</sup> By using a Duolink-PLA strategy, we could indeed confirm that VWF is unable to associate with LRP1 under static conditions (Figure 1). In contrast, when macrophages were analyzed via classical immune-fluorescent staining, the presence of VWF on THP1-derived macrophages could readily be detected (Figure 1). These data are in agreement with previous

observations from our laboratory, in which we have observed VWF staining on primary monocyte-derived macrophages.<sup>17,28</sup> It should be noted that Castro-Nunez and colleagues were unable to detect VWF binding to macrophages under static conditions.<sup>26</sup> The lack of VWF detection may be related to the conditions in which the macrophages were cultured. Alternatively, their method requires perhaps higher VWF concentrations for binding to become detectable.

Macrophages express a number of candidate receptors that can be involved in VWF binding, including Siglec-5 and the asialoglycoprotein receptor. Nevertheless, their relative contribution to VWF clearance remains unclear, and is probably modest at best under regular physiological conditions. In this study, we focused on SR-AI (also known as SCARA1 or CD204) as a novel candidate receptor that is specifically expressed in macrophages and dendritic cells. The interest in this receptor mainly originates from its high structural homology with SCARA5, an epithelial receptor that has been identified in genome-wide association studies to be associated with VWF plasma levels.<sup>24</sup> SR-AI and SCARA5 are both single transmembrane scavenger receptors that interact with their ligands via an ectodomain that consists of a collagenous domain and three scavenger receptor cysteine-rich domains.<sup>29</sup> The potential of SR-AI to interact with VWF became evident in solid-phase binding experiments, in which saturable and dose-dependent binding was observed (Figure 2). It was remarkable to note that half-maximal binding was obtained at  $3.5 \mu\text{g/mL}$  VWF, corresponding to  $14 \text{ nM}$ . Although our experimental approach in combination with the multimeric structure does not allow the calculation of a true affinity constant, this value suggests that VWF is able to interact with SR-AI with relatively high affinity. This value is considerably lower than the apparent affinity constants we recently identified for the interactions of SR-AI with factor X and pentraxin-2 ( $0.7 \mu\text{M}$  and  $0.2 \mu\text{M}$ , respectively), suggesting that VWF binds to SR-AI more efficiently than factor X and pentraxin-2. It is worth mentioning that, in direct competition experiments, VWF was unable to displace factor X from SR-AI (*data not shown*), indicating that both ligands bind to distinct interactive sites on SR-AI. This possibility fits with the notion that factor X binding is cation-independent (*data not shown*), whereas VWF binding is fully cation-dependent (Figure 2). Possibly, VWF binding involves similar regions within SR-AI that also mediate the cation-dependent cell adhesion.<sup>25</sup>

With regard to VWF, the interaction with SR-AI appears to involve multiple regions within the VWF molecule, including at least the D'D3-region, the A1 domain and the D4 domain (Figure 2). While testing a library of  $>20$  monoclonal anti-VWF antibodies, we identified two antibodies that were able to interfere with the interaction between VWF and SR-AI (Figure 2). One is directed against the A1 domain (MAb723) and the other against the D4 domain (MAb540), which is in agreement with the involvement of multiple VWF regions contributing to the interaction with SR-AI. It is important to mention here that preliminary studies in our laboratory revealed that the D'D3-region and the D4 domain also contain binding sites for LRP1 (*data not shown*). Thus, there seems to be an overlap in domains involved in binding to SR-AI and LRP1. Nevertheless, the interaction of VWF with SR-AI is most likely distinct from its interaction with LRP1. First, antibodies MAb723 and MAb540 do not affect binding of

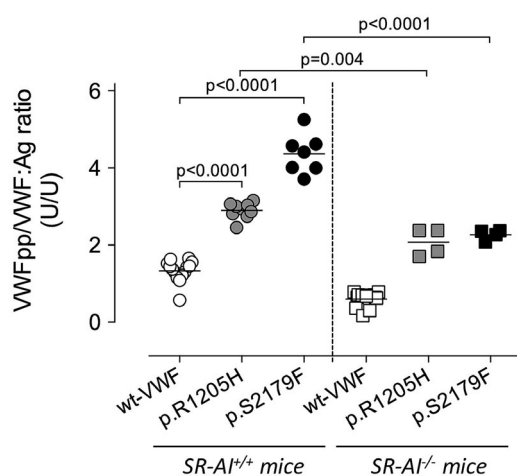


**Figure 7. SR-AI-deficiency is associated with decreased VWFpp/VWF:Ag ratios for mutants p.R1205H and p.S2179F.** Mutants VWF/p.R1205H and VWF/p.S2179F were expressed in SR-AI-expressing control mice and in SR-AI-deficient mice following hydrodynamic gene transfer. Four days after injection, plasma samples were prepared for the analysis of VWFpp and VWF:Ag. VWFpp/VWF:Ag ratios for each individual mouse included in the study are plotted. Data for wt-VWF are similar to those presented in Figure 5. Statistical analysis involved one-way ANOVA followed by the Tukey multiple comparison test.



VWF to LRP1 (*data not shown*), indicating that binding sites in these domains do not overlap. Second, introduction of the VWD-type 2B mutation leaves binding of VWF to SR-AI unaffected, as does the addition of ristocetin. Hence, VWF does not need to be in its active conformation to interact with SR-AI, whereas it does need to be for binding to LRP1. As for the role of glycans present on the VWF molecule in the interaction with SR-AI, this could be the subject of further studies. However, neither the A1 domain nor the D4 domain contains glycan structures, suggesting that the interaction with SR-AI is mainly glycan-independent. This does not exclude the possibility that glycans elsewhere in the protein could modulate this interaction, akin to what has previously been reported for the binding of the A1 domain to LRP1.<sup>11</sup>

Apart from binding to purified recombinant soluble SR-AI, we also observed a specific binding of VWF to cellular SR-AI (Figure 3). First, we used SR-AI-transfected HEK293 cells as a model system, and both classical immunofluorescent staining and the Duolink-PLA revealed selective binding of VWF to SR-AI. Second, the association of VWF with THP1-derived macrophages (as depicted in Figure 1) is at least in part mediated by SR-AI, as illustrated by the Duolink-PLA approach (Figure 3). Moreover, immunostaining for VWF on THP1-derived macrophages was strongly reduced in the presence of antibodies Mab723 and Mab540, which interfere with SR-AI binding (Figure 4). Finally, when binding of VWF to primary bone marrow-derived murine macrophages was tested, binding was reduced to near background levels for SR-AI-deficient macrophages compared to wt-macrophages (Figure 4). Being able to interact with SR-AI expressed on the cell surface supports a role of SR-AI as a clearance receptor for VWF. We analyzed this possibility by measuring VWFpp/VWF:Ag ratios of human VWF expressed in wt- and SR-AI-deficient mice. There were several reasons for choosing this approach over measuring classical VWF survival. First, in a recent study we compared the clearance of two mutants in parallel via protein survival and via measuring VWFpp/VWF:Ag ratios.<sup>9</sup> This analysis revealed that the VWFpp/VWF:Ag approach was clearly more sensitive than the classic protein survival experiments in detecting differences in VWF clearance, due to a markedly smaller error margin between mice. Second, this smaller error margin also favors the use of fewer mice in this type of experiments. For a classical clearance experiment, approximately 15 mice are included per molecule to be tested, whereas with the VWFpp/VWF:Ag approach fewer than ten mice per molecule are needed. Thus, from an animal ethical perspective this latter approach is to be preferred. Finally, expression in hepatocytes allows more homogeneous post-translational processing compared to the production of proteins in distinct stable cells lines. Indeed, the lectin binding profile of hepatic VWF is similar to that of endothelial VWF.<sup>30</sup> One might fear interference of clearance of hepatic VWF by endogenous endothelial-derived VWF. However, VWF clearance is similar in wt- and VWF-deficient mice,<sup>3</sup> and even at VWF levels of 1500%, clearance remains unsaturated.

Compared to VWFpp/VWF:Ag ratios obtained for wt-mice (ratio=1.3) and LRP1-deficient mice (ratio=1.1), these ratios were strongly reduced in SR-AI-deficient mice (ratio=0.6). This not only points to SR-AI being a clearance

receptor for VWF, but also to SR-AI being more dominant in VWF clearance than LRP1. We anticipated that endogenous VWF levels would be increased in SR-AI-deficient mice compared to those in wt-mice. However, analysis of VWF levels did not reveal a statistically significant difference between SR-AI-deficient and wt-mice. We believe that the lack of difference is due to the fact that the SR-AI-deficient and wt-mice were not true littermates, which complicates a direct comparison. Indeed, even among mice with a similar genetic background, the variation in VWF levels is substantial (e.g. 0.3-1.9 U/mL),<sup>12,31</sup> which may explain the lack of difference between SR-AI-deficient and wt-mice. Of note, we observed that murine VWF efficiently interacts with murine SR-AI, indicating that the lack of difference is not because murine VWF is unable to interact with this receptor.

An intriguing aspect of VWF receptor interactions is how these are modulated by mutations in VWF, in particular those mutations that are associated with increased clearance. We previously showed that VWD-type 2B mutations promote spontaneous binding to LRP1, explaining the increased clearance of these mutants. Here we examined two clearance mutants: VWF/p.R1205H and VWF/p.S2179F.<sup>1,3,5,8</sup> Both mutants are known to be associated with increased VWFpp/VWF:Ag ratios; in humans for VWF/p.S2179F and in human and mice for VWF/p.R1205H.<sup>5,7,8</sup> Here we show that both mutants display increased binding to SR-AI, both to purified SR-AI and SR-AI expressed on THP1-cells (Figure 6). Increased binding of the VWF/p.R1205H is in agreement with data reported by O'Donnell *et al.*, who also observed increased binding of this mutant to macrophages. Increased binding to SR-AI may suggest that SR-AI contributes to the accelerated removal of these mutants from the circulation. Indeed, VWFpp/VWF:Ag ratios for VWF/p.R1205H and VWF/p.S2179F were significantly reduced in SR-AI-deficient mice compared to wt-mice (Figure 7). However, even in the SR-AI-deficient mice, these ratios were substantially higher compared to wt-VWF, indicating that SR-AI is not the only receptor that mediates increased clearance of these mutants. We considered the option that LRP1 could play a role in the enhanced clearance of these mutants, and preliminary experiments revealed that both mutants did indeed display enhanced binding to LRP1 (*data not shown*). Apparently, enhanced receptor binding due to such clearance mutations is not always restricted to a single receptor, but may involve several receptors simultaneously, thereby multiplying the clearance rate of the mutant proteins.

In summary, we identify SR-AI as a macrophage-specific receptor for VWF, and this receptor may contribute to the increased clearance of certain VWF clearance mutants.

#### Acknowledgments

This study was supported by grants from the Agence Nationale de la Recherche (ANR-13-BSV1-0014; PJJ), and the Fondation pour la Recherche Médicale (FRM-SPF20130526717; NW & PJJ). We would like to thank Pascal Roux & Dr. Audrey Salles (Pasteur Institute, Paris, France) for their help in accessing the confocal microscope facility and interpretation of optical microscopy data and Emilie Bouvier & Alexandre Diet (Center for Breeding & Distribution of Transgenic Animals, Orléans, France) for their technical assistance.

## References

- Casonato A, Pontara E, Sartorello F, et al. Reduced von Willebrand factor survival in type Vicenza von Willebrand disease. *Blood*. 2002;99(1):180-184.
- Haberichter SL, Castaman G, Budde U, et al. Identification of type 1 von Willebrand disease patients with reduced von Willebrand factor survival by assay of the VWF propeptide in the European study: molecular and clinical markers for the diagnosis and management of type 1 VWD (MCMDM-1VWD). *Blood*. 2008;111(10):4979-4985.
- Lenting PJ, Westein E, Terraube V, et al. An experimental model to study the in vivo survival of von Willebrand factor. Basic aspects and application to the R1205H mutation. *J Biol Chem*. 2004;279(13):12102-12109.
- van Schooten CJ, Tjernberg P, Westein E, et al. Cysteine-mutations in von Willebrand factor associated with increased clearance. *J Thromb Haemost*. 2005;3(10):2228-2237.
- Haberichter SL, Balistreri M, Christopherson P, et al. Assay of the von Willebrand factor (VWF) propeptide to identify patients with type 1 von Willebrand disease with decreased VWF survival. *Blood*. 2006;108(10):3344-3351.
- Sztukowska M, Gallinaro L, Cattini MG, et al. Von Willebrand factor propeptide makes it easy to identify the shorter von Willebrand factor survival in patients with type 1 and type Vicenza von Willebrand disease. *Br J Haematol*. 2008;143(1):107-114.
- Eikenboom J, Federici AB, Dirven RJ, et al. VWF propeptide and ratios between VWF, VWF propeptide, and FVIII in the characterization of type 1 von Willebrand disease. *Blood*. 2013;121(12):2336-2339.
- Pruss CM, Golder M, Bryant A, et al. Pathologic mechanisms of type 1 VWD mutations R1205H and Y1584C through in vitro and in vivo mouse models. *Blood*. 2011;117(16):4358-4366.
- Wohner N, Legendre P, Casari C, Christophe OD, Lenting PJ, Denis CV. Shear stress-independent binding of von Willebrand factor-type 2B mutants p.R1306Q & p.V1316M to LRP1 explains their increased clearance. *J Thromb Haemost*. 2015;13(5):815-820.
- O'Sullivan JM, Aguila S, McRae E, et al. N-linked glycan truncation causes enhanced clearance of plasma-derived von Willebrand factor. *J Thromb Haemost*. 2016;14(12):2446-2457.
- Chion A, O'Sullivan JM, Drakeford C, et al. N-linked glycans within the A2 domain of von Willebrand factor modulate macrophage-mediated clearance. *Blood*. 2016;128(15):1959-1968.
- Rastegarlarlari G, Pegon JN, Casari C, et al. Macrophage LRP1 contributes to the clearance of von Willebrand factor. *Blood*. 2012;119(9):2126-2134.
- Grewal PK, Uchiyama S, Ditto D, et al. The Ashwell receptor mitigates the lethal coagulopathy of sepsis. *Nat Med*. 2008;14(6):648-655.
- Rydz N, Swystun LL, Notley C, et al. The C-type lectin receptor CLEC4M binds, internalizes and clears von Willebrand factor and contributes to the variation in plasma von Willebrand factor levels. *Blood*. 2013;121(26):5228-5237.
- Pegon JN, Kurdi M, Casari C, et al. Factor VIII and von Willebrand factor are ligands for the carbohydrate-receptor Siglec-5. *Haematologica*. 2012;97(12):1855-1863.
- Casari C, Lenting PJ, Wohner N, Christophe OD, Denis CV. Clearance of von Willebrand factor. *J Thromb Haemost*. 2013;11 Suppl 1:202-211.
- van Schooten CJ, Shahbazi S, Groot E, et al. Macrophages contribute to the cellular uptake of von Willebrand factor and factor VIII in vivo. *Blood*. 2008;112(5):1704-1712.
- Muczynski V, Ayme G, Regnault V, et al. Complex formation with pentraxin-2 regulates factor X plasma levels and macrophage interactions. *Blood*. 2017;129(17):2443-2454.
- Muczynski V, Bazaa A, Loubiere C, et al. Macrophage receptor SR-AI is crucial to maintain normal plasma levels of coagulation factor X. *Blood*. 2016;127(6):778-786.
- Breslin WL, Strohacker K, Carpenter KC, Haviland DL, McFarlin BK. Mouse blood monocytes: standardizing their identification and analysis using CD115. *J Immunol Methods*. 2013;390(1-2):1-8.
- Marx I, Christophe OD, Lenting PJ, et al. Altered thrombus formation in von Willebrand factor-deficient mice expressing von Willebrand factor variants with defective binding to collagen or GPIIb/IIIa. *Blood*. 2008;112(3):603-609.
- Marx I, Lenting PJ, Adler T, Pendu R, Christophe OD, Denis CV. Correction of bleeding symptoms in von Willebrand factor-deficient mice by liver-expressed von Willebrand factor mutants. *Arterioscler Thromb Vasc Biol*. 2008;28(3):419-424.
- Rayes J, Hollestelle MJ, Legendre P, et al. Mutation and ADAMTS13-dependent modulation of disease severity in a mouse model for von Willebrand disease type 2B. *Blood*. 2010;115(23):4870-4877.
- Smith NL, Chen MH, Dehghan A, et al. Novel associations of multiple genetic loci with plasma levels of factor VII, factor VIII, and von Willebrand factor: the CHARGE (Cohorts for Heart and Aging Research in Genome Epidemiology) Consortium. *Circulation*. 2010;121(12):1382-1392.
- Santiago-Garcia J, Kodama T, Pitas RE. The class A scavenger receptor binds to proteoglycans and mediates adhesion of macrophages to the extracellular matrix. *J Biol Chem*. 2003;278(9):6942-6946.
- Castro-Nunez L, Dienava-Verdoold I, Herczenik E, Mertens K, Meijer AB. Shear stress is required for the endocytic uptake of the factor VIII-von Willebrand factor complex by macrophages. *J Thromb Haemost*. 2012;10(9):1929-1937.
- van der Flier A, Liu Z, Tan S, et al. FcRn rescues recombinant factor VIII Fc fusion protein from a VWF independent FVIII clearance pathway in mouse hepatocytes. *PLoS One*. 2015;10(4):e0124930.
- Casari C, Du V, Wu YP, et al. Accelerated uptake of VWF/platelet complexes in macrophages contributes to VWD type 2B-associated thrombocytopenia. *Blood*. 2013;122(16):2893-2902.
- Zani IA, Stephen SL, Mughal NA, et al. Scavenger receptor structure and function in health and disease. *Cells*. 2015;4(2):178-201.
- Badirou I, Kurdi M, Legendre P, et al. In vivo analysis of the role of O-glycosylations of von Willebrand factor. *PLoS One*. 2012;7(5):e37508.
- Lemmerhirt HL, Broman KW, Shavit JA, Ginsburg D. Genetic regulation of plasma von Willebrand factor levels: quantitative trait loci analysis in a mouse model. *J Thromb Haemost*. 2007;5(2):329-335.